scientific reports

Check for updates

OPEN

Simulation of hybridized nanofluids flowing and heat transfer enhancement via 3-D vertical heated plate using finite element technique

Muhammad Bilal Hafeez[1]✉, Marek Krawczuk[1], Hasan Shahzad[2], Amjad Ali Pasha[3] & Mohammad Adil[4,5]

The present study probed the creation of heat energy and concentrating into Newtonian liquids across vertical 3D-heated plates. The role of the Soret and Dufour theories in concentrating and energy formulas is discussed. The role of hybrid nanoparticles is introduced to illustrate particle efficiency in terms of solute and thermal energy. It is removed a viscous dissipation process and a changing magnetic field. The proposed approach is motivated by the need to maximize solute and thermal energy uses in biological and industrial domains. The constructed system of (partial differential equations) PDEs includes concentration, momentum, and thermal energy equations within various thermal characteristics. Transformations are used to formulate the system of (ordinary differential equations) ODEs for solution. To assess various features vs various variables, a Galerkin finite element approach is used. Motion into nanoscale components is shown to be smaller than motion into hybrid nanoparticles. Furthermore, fluctuations in heat energy and solute particle counts are seen in relation to changes in Soret, Eckert, magnetic, and Dufour numbers. The basic finding is that the generation of thermal energy for hybridized nanomaterials is much higher.

List of symbols

Du	Dufour number
T	Temperature of nanofluid
T_∞	Ambient temperature
g^*	Gravitational force
u, v	Velocity component in x, y direction (ms^{-1})
D	Mass diffusion (coefficient)
Ec	Eckert number
k	Thermal conductivity
x, y, z	Dimensional space coordinates (m)
Pr	Prandtl number
Sr	Soret number
Sc	Schmidt number
K^*	Porous medium parameter
C_{fx}	Surface force

[1]Faculty of Mechanical Engineering and Ship Technology, Institute of Mechanics and Machine Design, Gdansk University of Technology, Narutowicza 11/12, 80-233 Gdańsk, Poland. [2]Faculty of Materials and Manufacturing, College of Mechanical Engineering and Applied Electronics Technology, Beijing University of Technology, Beijing, China. [3]Aerospace Engineering Department, King Abdulaziz University, Jeddah 21589, Saudi Arabia. [4]Mechanical Engineering Program, Physical Science and Engineering Division, King Abdullah University of Science and Technology, Thuwal 23955-6900, Saudi Arabia. [5]KAUST Clean Combustion Research Center, King Abdullah University of Science and Technology, Thuwal 23955-6900, Saudi Arabia. ✉email: Muhammad.bilal.hafeez@pg.edu.pl

Re	Reynolds number
M	Magnetic parameter
G-FEM	Galerkin finite element method
Nu	Nusselt number
PDEs	Partial differential equations
Ag	Silevr
Cu	Copper
Sh	Rate of mass diffusion
H_2O	Water
k	Thermal conductivity (W m^{-1} K^{-1})
q_w	Wall heat flux
h_{nf}	Hybrid nanoparticles

Greek symbols

ρ	Density
β^*	Heat source
ρc_p	Heat capacity
ϕ	Volume fractions
σ	Electrically conductivity (Ω m) $^{-1}$
D_{hnf}	Thermal diffusivity of the hybrid nanofluid
β_{hnf}	Volumetric thermal expansion number

Heat transfer is a thermal engineering subject that entails the manufacture, use, conversion, and alternate of warmth power among transportable structures. Heat transfer is split into diverse approaches, which include thermal conduction, thermal convection, thermal radiation, and energy transfer through section changes. Engineers additionally don't forget to shift an extensive variety of chemical compounds (advection mass switch), both bloodless or hot, to attain a heat switch. Although those techniques have unique characteristics, they generally arise concurrently withinside the identical system. Heat alternate happens while the waft of a huge quantity of liquid (fuel line or liquid) contains its warmth in a liquid. All convective approaches additionally transmit partial warmth to the circulation, as well[1]. Heat switch is one of the maximum vital commercial approaches. Throughout the economic field, warmth ought to be added, subtracted, or eliminated from the distribution of one technique to another. In theory, the heat dissipated through a hot liquid is in no way precisely similar to the heat received through a cold liquid because of the lack of herbal warmth[2]. Application for heat transfer in commercial manufacturing 99% of manufacturing makes use of a particular technique to transfer heat. Drying approaches are all types of heat transfer. The commercial makes use of heat transfer fluids vary, from simple, dry layouts to superior sized structures that carry out many features withinside the manufacturing technique. As there are numerous versions withinside the layout and alertness of approaches withinside the use of heat transfer fluids, the quantity of industries that use this technique is likewise huge[3]. Miniaturization has a large effect on the generation of heat exchangers and turns heat exchangers into an extra compact and extra green. The performance of the heat exchanger has an extremely good effect on the general performance and fitness of the thermal power system. The micro-channel heat sink is a brand new device in warmth alternate generation. The benefits of a huge heat transfer area and the excessive cohesiveness of a small channel heat sink make it a green warmth exchanger for the usage of electronic cooling[4].

Zahra et al.[5] investigated the effects of thermal radiation heat transfer with a solar system subjected to flow with nanoparticles. Sheikholeslami and Ganji[6] discussed heat transfer in ferrofluids with nanoparticles exposed to a magnetic field. Zeeshan and Bhargav[7] investigated the influence of dispersion of and in fluid on heat transfer in the fluid using the molecular dynamics approach. Sajjad et al.[8] analyzed the influence of the Darcy-Forchheimer porous medium and nanoparticles on heat transfer in fluid over a moving surface.

A hybrid material is a substance that mixes bodily and chemical properties of various substances concurrently and affords those homes in a homogeneous segment. Synthetic hybrid nanomaterials show off first-rate physicochemical homes that don't exist withinside the character components. An enormous quantity of studies has been finished concerning the homes of those composites[9] and hybrid substances which include carbon nanotubes (CNTs) had been utilized in electrochemical sensors, bio-sensors, nanocatalysts, etc.[10] however the use of those hybrid nanomaterials in nanofluids has now no longer advanced as such. Work on hybrid nanofluids could be very restricted and a whole lot of experimental look continues to be being finished. According to Makishima[11] while or greater substances are blended so that their aggregate has a specific chemical bond entitled "hybrid metals". In fact, while or greater metals added the homogeneous segment with simultaneous blending named "hybrid nanofluid". This superior elegance of nanofluids confirmed promising enhancement in heat transfer traits and thermophysical and hydrodynamic homes as compared to unitary nanofluids. Hayat and Nadeem[12] discovered that the hybrid nanofluid finished nicely with a better warmth switch charge as compared to unitary nanofluid even withinside the presence of heat generation, chemical reaction, and thermal radiation. They found this even as investigating the rotating three-d consistent waft of Ag–CuO/water hybrid nanofluid. Selimefendigil and Öztop[13] compared the thermal overall performance of TiO_2, Cu, and Al_2O_3 and located that Cu nanofluids furnished relatively higher results. Azmi et al.[14] deliberated the hybrid nanofluids thermophysical homes, education methods, a current development, and execution outcomes on heat transfer, friction factor, and stress drop. Minea et al.[15] mentioned the programs of hybrid nanofluids in solar power with the guidance of a few debates on thermophysical homes and mathematical modeling which include numerical details. Nazir et al.[16]

discussed the role of Williamson liquid in thermal energy and concentration involving hybrid nanoparticles toward melting surfaces via non-Fourier's theory. Dogonchi et al.[17] analyzed the role of hybrid nanoparticles on the thermal efficiency of fluid between two parallel plates subjected to thermal radiation. Chamkha et al.[18] published on the simultaneous influence of hybrid nanoparticles, magnetic fields, and rotations of walls on the transfer of heat. Masayebidarched et al.[19] performed theoretical analysis for the thermal enhancement in fluid with hybrid nanoparticles. Similar works published on the role of hybrid nanoparticles on thermal enhancement can be seen in references[20–32].

To conclude, the latest development on the simultaneous transfer of heat and mass has revealed that compositional gradients are a favorable factor for the transfer heat. Similarly, a temperature gradient is supported to enhance mass transfer in fluids. The transfer of heat due to compositional differences of solute is termed the Dufour effect, whereas the transfer of mass due to temperature gradient is called the Soret effect. These effects have been studied theoretically in recent years. For instance, Hayat and Nawaz[33] studied the combined effects of temperature and concentration gradients on mixed convection heat and mass transport in partially ion, second grade fluid subjected to a magnetic field. Nawaz et al.[34] studied the Soret and Dufour effects on heat and mass transfer in an axisymmetric flow between two moving surfaces. Subrat et al.[35] examined the Soret and Dufour effects on the transport phenomenon in thermochemical flow. Iskandar et al.[36] analyzed the combined effects of Soret and Dufour due to the suspension of nanosized particles on heat and mass transfer in flow over a moving thin needle. Ambreen et al.[37] also examined the impact of temperature and concentration gradients.

Recently extensive studies paintings have been completed on the fluid's dynamics withinside the presence of a magnetic field. The effects of the magnetic discipline on fluids are well worth investigating because of its several packages in a huge variety of fields. The examination of the interplay of the magnetic discipline or the electromagnetic discipline on fluids has been documented, e.g., in nuclear fusion, chemical engineering, medication, and transformer cooling. A magnetic nanofluid (ferrofluid) is a magnetic colloidal suspension along with a base liquid and magnetic nanoparticles with a length variety of 5–15 nm in diameter coated with a surfactant layer Sheikholeslami and Rashidi[38], Ganguly et al.[39] studied the impact of a line dipole on warmth switch enhancement. They located that an enhancement withinside the general heat switch relies upon the internet magnetizing cutting-edge in addition to the relative placement of the dipoles. Parsa et al.[40] investigated the magneto-hemodynamic laminar viscous glide of an accomplishing physiological fluid in a semi-porous channel beneath neath a transverse magnetic discipline. Sheikholeslami and Ellahi[41] studied 3-dimensional mesoscopic simulation of magnetic discipline impact on herbal convection of nanofluid. They located that thermal boundary layer thickness growth with growth withinside the Lorentz force. The vortex dynamics in the back of diverse magnetic limitations and traits of warmth switches have been investigated by Zhang and Huang[42]. They located that the stress drop penalty isn't depending on the interplay parameter. Nanofluid glide and heat transfer traits among horizontal parallel plates in a rotating gadget have been investigated by Sheikholeslami et al.[43]. They located that the Nusselt range will increase with a growth in nanoparticle quantity fraction and the Reynolds range; however, it decreases with a growth withinside the Eckert range, the magnetic and the rotation parameters. Ghofrani et al.[44] provided experimental research on pressured convection warmth switch of an aqueous ferrofluid glide passing thru a round copper tube withinside the presence of an alternating magnetic discipline. They located that the impact of the magnetic discipline in low Reynolds numbers is higher, and a most of 27.6% enhancement withinside the convection heat transfer is observed. Sheikholeslami et al.[45] used lattice Boltzmann simulation (LBM) to simulate nanofluid glide and heat transfer outcomes in a horizontal cylindrical enclosure with an internal triangular cylinder. Rashidi et al.[46] studied the results of magnetic interplay range, slip component, and relative temperature distinction on velocity and temperature profiles in addition to entropy technology in Magnetohydrodynamic (MHD) glide of a fluid over a rotating disk with variable properties[47–57]. include new additions that consider conventional and hybrid nanofluids with heat and mass transmission in a variety of physical circumstances.

The unique connections among thermophysical parameters, no previous study on thermal enhancement and mass transposition in three-dimensional Newtonian liquids flowing across vertical heated plates have been investigated. It is found that the basis liquids of the hybrid nanofluids tested include copper (Cu), silver (Ag), and water (H_2O). Following the similarity approach, numerical solutions are obtained using the robust Galerkin finite element technique for the controlling PDEs system. Hybrid nanofluid passes through vertical heated plates and offers a wide range of industrial applications, including coating and suspensions, cooling of metallic plates, heat exchanger technology, and materials processing. Manufacturing of aerodynamically extruded plastic sheets, the production of paper, heat-treated materials were going between feed and winding-up rolls, and the cooling of an endless metallic plate in a cooling bath.

For this reason, this research comprises five sections, each of which presents a variety of alternative answers. Section "Flow analysis" lays out the specifics of the issue at hand. Meanwhile, an overview of the numerical approach is provided in section "Numerical method and code validation". Section "Results and discussion" discusses the results. Section "Core points and conclusions" wraps up this investigation.

Flow analysis

The features of thermal energy and solute particles in Newtonian liquid inserting hybrid nanostructures toward a heated vertical surface are considered under the impact of a variable magnetic field. A porous surface is taken to characterize the motion and thermal energy of particles along with the Dufour and Soret influences. The composite of *Ag* and *Cu* is called a hybrid nanostructure, while *Ag* is known as a nanoparticle. The thermal properties of *Ag* and *Cu* are illustrated in Table 1.

Properties	Cu-Ag- polymer
Density (ρ)	$\rho_{hnf} = (1-\varphi)\rho_f + \varphi\rho_s$
Heat capacity (ρc_p)	$(\rho c_p)_{hnf} = [(1-\varphi)\rho_f + \varphi\rho_s][(1-\varphi)c_{pf} + \varphi c_{ps}]$
Viscosity (μ)	$\mu_{hnf} = (1-\varphi)^{-2.5}\mu_f$
Thermal conductivity (K)	$K_{hnf} = \left[\frac{k_1+(n_1-1)k_f-(n_1-1)\varphi_1(k_f-k_1)}{k_1+(n_1-1)k_f+\varphi_1(k_f-k_1)}\right] \times \left[\frac{k_1+(n_1-1)k_f-(n_1-1)\varphi_1(k_f-k_1)}{k_1+(n_1-1)k_f+\varphi_1(k_f-k_1)}\right] \times k_f$
Thermal diffusivity (D_{hnf})	$D_{hnf} = (1-\varphi)d_f$
Electrical conductivity (σ_{hnf})	$\sigma_{hnf} = \left[\frac{\sigma_2+2\sigma_{nf}-2\varphi_2(\sigma_{nf}-\sigma_2)}{\sigma_2+2\sigma_{nf}+\varphi_2(\sigma_{nf}-\sigma_2)}\right]\left[\frac{\sigma_1+2\sigma_f-2\varphi_1(\sigma_f-\sigma_1)}{\sigma_1+2\sigma_f+\varphi_1(\sigma_f-\sigma_1)}\right]$

Table 1. Correlation among hybrid nanostructures and nanomaterials in polymers.

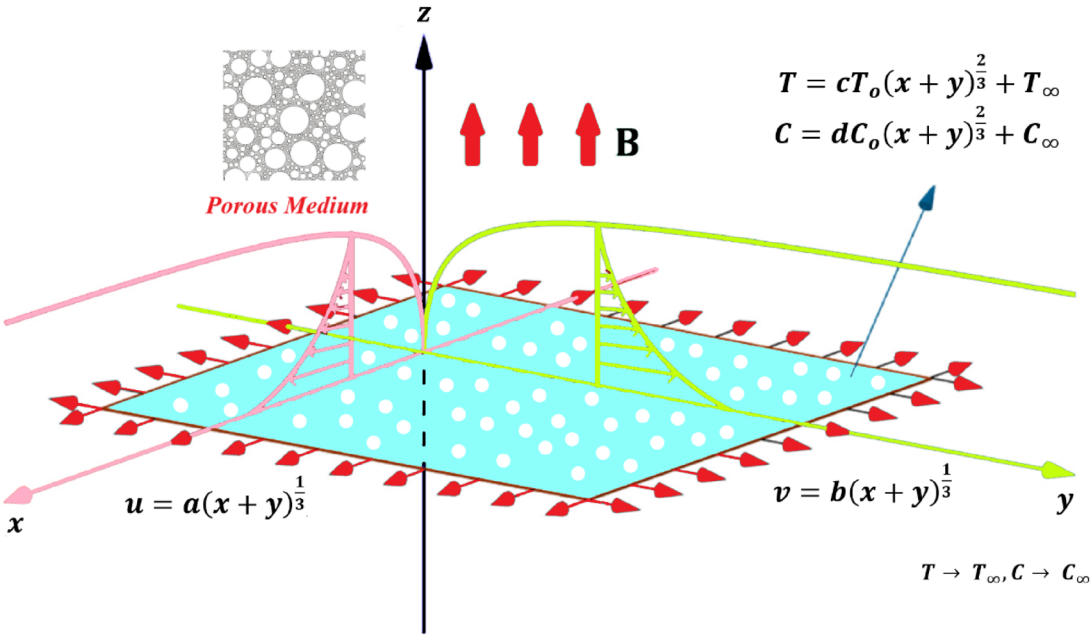

Figure 1. Geometry of hybrid nanostructures.

Assumptions of the current problem. Following suppositions and requirements are observed for the mathematical model:

- Hybrid nanofluid model
- Copper (Cu) and silver (Ag) nanoparticles
- Water (H_2O)as base fluid
- Magnetic field
- Porous media
- Heat source
- Vertical 3D-heated plates

The schematic behavior of the current model is presented in Fig. 1.

In Fig. 1, It noticed that x-axis is taken along vertical direction and y-axis is assumed along horizontal direction while magnetic field is inserted along y-direction. Magnetic field parameter reduces motion of particles. The flow region is exposed by taking a uniform transverse magnetic field and the maximum amount of thermal energy is achieved versus argument values of Eckert number, bouncy parameter and magnetic parameter.

PDEs, describing the problem[58,59], can be stated as

$$\frac{\partial u}{\partial x} + \frac{\partial v}{\partial y} + \frac{\partial w}{\partial z} = 0, \tag{1}$$

$$v\frac{\partial u}{\partial y}+w\frac{\partial u}{\partial z}+u\frac{\partial u}{\partial x}=\nu_{hnf}\frac{\partial^2 u}{\partial z^2}+\left(\beta_{hnf}\right)_T g^*(T-T_\infty)+\left(\beta_{hnf}\right)_C g^*(C-C_\infty)-\frac{\sigma_{hnf}}{\rho_{hnf}}B_o^2A^2(x+y)^{-\frac{2}{3}}u-\mu_{hnf}\frac{u}{K_1} \tag{2}$$

$$u\frac{\partial v}{\partial x}+v\frac{\partial v}{\partial y}+w\frac{\partial v}{\partial z}=\nu_{hnf}\frac{\partial^2 v}{\partial z^2}+\left(\beta_{hnf}\right)_T g^*(T-T_\infty)+\left(\beta_{hnf}\right)_C g^*(C-C_\infty)-\frac{\sigma_{hnf}}{\rho_{hnf}}B_o^2A^2(x+y)^{-\frac{2}{3}}v-\mu_{hnf}\frac{v}{K_1} \tag{3}$$

$$u\frac{\partial T}{\partial x}+v\frac{\partial T}{\partial y}+w\frac{\partial T}{\partial z}=\frac{K_{hnf}}{\left(\rho c_p\right)_{hnf}}\frac{\partial^2 T}{\partial z^2}+\frac{Q_0}{\left(\rho c_p\right)_{hnf}}(T-T_\infty)+\frac{DK_T}{C_sC_p}\frac{\partial^2 C}{\partial z^2}-\frac{\sigma_{hnf}}{\rho_{hnf}}B_o^2A^2(x+y)^{-\frac{2}{3}}v-\mu_{hnf}\frac{v}{K_1} \tag{4}$$

$$u\frac{\partial C}{\partial x}+v\frac{\partial C}{\partial y}+w\frac{\partial C}{\partial z}=(D)_{hnf}\frac{\partial^2 C}{\partial z^2}+\frac{D_T}{T_\infty}\frac{\partial^2 T}{\partial z^2}, \tag{5}$$

For system Eqs. (1)–(5) the BCs are (see for details,[58,59])

$$\left.\begin{gathered}u=U_w\left(=a(x+y)^{\frac{1}{3}}\right),v=b(x+y)^{\frac{1}{3}},w=0\\ T=T_w\left(=cT_o(x+y)^{\frac{2}{3}}+T_\infty\right),C=C_w\left(=dC_o(x+y)^{\frac{2}{3}}+C_\infty\right)\ as\ y=0\\ u=0,v=0,T\to T_\infty,C\to C_\infty\ as\ y\to\infty\end{gathered}\right\} \tag{6}$$

In the above equations, the velocity is $[u, v, 0]$, g^* denotes the gravitational force, $\rho$is the fluid density, μ is the kinematic viscosity, σ is the electrical conductivity, c_p is called the specific heat, k is the thermal conductivity, D is the mass diffusion (coefficient), and hnf is revealed by the hybrid nanostructures. It should be noted that a uniform magnetic field is taken along the z-direction of the surface while the flow runs due to stretching walls.

Table 1 demonstrates the composite relation between hybrid nanostructures and nanomaterials in polymers, which is called the base fluid.

In Table 1 the following denotes

$$\begin{gathered}\frac{K_{hnf}}{K_f}=\frac{k_1+(n_1-1)k_f-(n_1-1)\varphi_1(k_f-k_1)}{k_1+(n_1-1)k_f+\varphi_1(k_f-k_1)},\frac{\sigma_{nf}}{\sigma_f}=\frac{\sigma_1+2\sigma_f-2\varphi_1(\sigma_f-\sigma_1)}{\sigma_1+2\sigma_f+\varphi_1(\sigma_f-\sigma_1)},\\ \varphi=\frac{\frac{w_1+w_2}{\rho_s}}{\frac{w_1+w_2}{\rho_s}+\frac{w_f}{\rho_f}},\varphi_1=\frac{\frac{w_1}{\rho_1}}{\frac{w_1}{\rho_1}+\frac{w_2}{\rho_2}+\frac{w_f}{\rho_f}},\quad\varphi_2=\frac{\frac{w_2}{\rho_2}}{\frac{w_1}{\rho_1}+\frac{w_2}{\rho_2}+\frac{w_f}{\rho_f}},\\ \rho_s=\frac{(\rho_1\times w_1)(\rho_2\times w_2)}{w_1+w_2},\left(c_p\right)_s=\frac{\left(\left(c_p\right)_1\times w_1\right)\left(\left(c_p\right)_2\times w_2\right)}{w_1+w_2},\end{gathered} \tag{7}$$

Next, the similarity transformation is

$$\left.\begin{gathered}u=a(x+y)^{\frac{1}{3}},v=a(x+y)^{\frac{1}{3}},\eta=\sqrt{\frac{a}{\nu_f}}(x+y)^{-\frac{1}{3}}z,\\ w=-\sqrt{a\nu_f}(x+y)^{-\frac{1}{3}}\left(\frac{2}{3}(f+g)-\frac{1}{3}\eta(f'+g')\right),\theta=\frac{T-T_\infty}{T_w-T_\infty},\phi=\frac{C-C_\infty}{C_w-C_\infty}\end{gathered}\right\} \tag{8}$$

Consequently, using similarity transformation in Eqs. 1–6, we have

$$\left.\begin{gathered}\frac{\nu_{hnf}}{\nu_f}f'''-\frac{1}{3}(f'+g')f'+\frac{2}{3}(f+g)f''+(Gr)_t\theta\\ +(Gr)_c\phi-\left(\frac{\sigma_{hnf}}{\sigma_f}\right)\left(\frac{\rho_f}{\rho_{hnf}}\right)Mf'-\left(\frac{\mu_{hnf}}{\mu_f}\right)K^*f'=0\\ f'(0)=1,f(0)=0,\quad f'(\infty)\to 0,\end{gathered}\right\}$$
$$\left.\begin{gathered}\frac{\nu_{hnf}}{\nu_f}g'''-\frac{1}{3}(f'+g')g'+\frac{2}{3}(f+g)g''+(Gr)_t\theta\\ +(Gr)_c\phi-\left(\frac{\sigma_{hnf}}{\sigma_f}\right)\left(\frac{\rho_f}{\rho_{hnf}}\right)Mg'-\left(\frac{\mu_{hnf}}{\mu_f}\right)K^*g'=0\\ g'(0)=\beta,g(0)=0,\quad g'(\infty)\to 0,\end{gathered}\right\} \tag{9}$$

Physical property	Water	Cu	Ag
$\rho(Kg/m^3)$	997.1	8933	10,500
$k(\frac{W}{m.K})$	0.613	401	429
$c_p\left(\frac{J}{kg.K}\right)$	4179	385	429
$\sigma(\frac{\Omega}{m})$	0.05	5.96×10^7	6.3×10^7

Table 2. Thermal properties of water, copper and silver.

$$\left.\begin{array}{c}\left(\frac{K_{hnf}}{K_f}\right)\theta'' + \left(\frac{(\rho c_p)_{hnf}}{(\rho c_p)_f}\right)\frac{2}{3}Pr(f+g)\theta' - \left(\frac{(\rho c_p)_{hnf}}{(\rho c_p)_f}\right)\frac{2}{3}Pr(f'+g')\theta \\ -Pr\beta^*\theta + \left(\frac{(\rho c_p)_{hnf}}{(\rho c_p)_f}\right)DuPr\phi'' + \left(\frac{\sigma_{hnf}}{\sigma_f}\right)MPrEc(f'+g')^2 = 0 \\ \theta(0)=1, \quad \theta(\infty)\to 0\end{array}\right\},$$
$$\left.\begin{array}{c}\left(\frac{D_{hnf}}{D_f}\right)\phi'' + \frac{2}{3}Sc(f+g)\phi' - \frac{2}{3}Sc(f'+g')\phi + SrSc\theta'' = 0 \\ \phi(0)=1, \quad \phi(\infty)\to 0\end{array}\right\}. \tag{10}$$

where, the following denotes: (Dufour number) Du, (Eckert number) Ec, Soret number (Sr), (Schmidt number) Sc, (Prandtl number) Pr, (porous medium parameter) (K^*), (volumetric thermal expansion number) β_{hnf}, (heat generation) β^*, (Grashof number) $(Gr)_c$ and (magnetic parameter) M. The dimensionless numbers and defined here

$$\left.\begin{array}{c}(Gr)_t = \frac{(\beta_{hnf})_T g^* cT_0}{a^2}, (Gr)_c = \frac{(\beta_{hnf})_C g^* dC_0}{a^2}, M = \frac{\sigma_f}{\rho_f}\frac{B_0^2 A^2}{a}, K^* = \frac{\mu_f}{ak_1} \\ Ec = \frac{1}{(c_p)_f}\frac{a^2}{cT_0}, \beta^* = \frac{Q_0}{a(\rho c_p)_f}, Du = \frac{DK_T dC_0}{C_s C_p V_f cT_0}, Sc = \frac{V_f}{d_f}, Sr = \frac{D_T T_0}{(T_\infty C_0)V_f}.\end{array}\right\}$$

The practical proposed model parameters used in this study are summarized in Table 2.
The surface forces are captured as

$$C_{fx} = \frac{\frac{\partial u}{\partial z}\big|_{z=0}}{\rho_f (U_w)^2} = \frac{(1-\phi)^{-2.5}}{(Re)^{1.5}} f''(0), \tag{11}$$

$$C_{gy} = \frac{\frac{\partial v}{\partial z}\big|_{z=0}}{\rho_f (U_w)^2} = \frac{-(1-\phi)^{2.5}}{(Re)^{1.5}} g''(0). \tag{12}$$

Nusselt number is

$$Nu = -\frac{(x+y)K_{hnf}\frac{\partial T}{\partial y}\Big|_{y=0}}{k_f(T-T_\infty)} = -\frac{K_{hnf}}{k_f (Re)^{1.5}}\theta'(0), \tag{13}$$

the rate of mass diffusion is

$$Sh = \frac{(x+y)D_{hnf}\frac{\partial C}{\partial y}\Big|_{y=0}}{D_f(C-C_\infty)} = -\frac{D_{hnf}}{D_f (Re)^{1.5}}\phi'(0), \tag{14}$$

where, $Re = \frac{xU_w}{\nu_f}$, the Reynolds number.

Numerical method and code validation

The G-FEM (Galerkin finite element method)[60–64] is used via COMSOL Multiphysics calculation software to obtain the solution of the presented problem. The working rules of G-FEM are given below:

- The residual equations are constructed.
- The residual is integrated over the typical element of the discretized domain.
- The weighted residual integrals are approximated using the Galerkin approach, and stiffness matrices are derived.
- The rules of assembly of elements are followed, and a nonlinear system of equations is linearized. The linearized system is solved under computational tolerances 10^{-3}.
- The convergence is checked, and grid-independent results are obtained. The criterion of error analysis is used.

Division of elements	$f'\left(\frac{\eta_{max}}{2}\right)$	$g'\left(\frac{\eta_{max}}{2}\right)$	$\theta\left(\frac{\eta_{max}}{2}\right)$
30	0.49906667	0.443556676	0.055501654
60	0.88512223	0.872840112	0.345670987
90	0.62693678	0.621570046	0.058457122
120	0.59438123	0.509121334	0.057888099
150	0.59196567	0.497570987	0.057527446
180	0.60400213	0.592340987	0.057229098
210	0.61009098	0.509400003	0.056238099
240	0.60424098	0.499011223	0.056821432
270	0.50980001	0.507710098	0.058645667
300	0.59632222	0.506367767	0.056854098

Table 3. Mesh-free investigation of temperature and velocities within 300 elements.

	Ref.[65]	Ref.[66]	Present study
	0.68	0.681052103137	0.681052103137
	0.72141	0.723331807103	0.723331807103
K_{nf}	0.82458	0.824720819103	0.824720819103

Table 4. In the case of nanofluids, the temperature changes were compared to the reported data of Ref.[65] and Ref.[66].

	Ø	*Knf*	*vf*	*Du*	Pr	*Sc*	*β*	
Ag								
	0.05	0.709 3	7.73×10^{-7}	4.452	61 5.45	8.6×10^{-7}	4.8×10^{-7}	
	0.01	0.631 5	9.54×10^{-7}	6.287	68 5.83	2.2×10^{-7}	1.2×10^{-7}	
Cu								
	0.03	0.669 6	8.75×10^{-7}	5.418	66 1.57	7.3×10^{-7}	3.7×10^{-7}	
	0.05	0.709 3	8.17×10^{-7}	4.758	65 0.81	1.2×10^{-6}	6.3×10^{-7}	
Ø	***Ag* Nanofluids**		***Cu* Nanofluids**		***Ag* Hybrid nanofluids**		***Cu* Hybrid nanofluids**	
	Numeric	Analytic	Numeric	Analytic	Numeric	Analytic	Numeric	Analytic
For different types of nanoparticles and hybrid particles								
0.1	1.011 1	1.011 0	1.011 0	1.010 9	1.007 1	1.006 6	1.009 3	1.008 9
0.3	1.032 7	1.032 3	1.032 6	1.032 1	1.020 9	1.019 3	1.027 7	1.026 3
0.5	1.054 6	1.053 6	1.543 9	1.053 5	1.035 3	1.032 9	1.046 2	1.044 2

Table 5. Nanofluid properties and non-dimensional parameters as function of type and volume fraction of nanoparticles and hybrid nanoparticles.

$$\left|\frac{\eta_{i+1}-\eta_i}{\eta^i}\right| < 10^{-5}. \tag{15}$$

- Table 3 reveals the investigation of mesh-free;
- Convergence analysis is confirmed via 300 elements.

In examples, a parametric study is elaborated to study heat energy and mass transfer in 3D flow of Newtonian fluid, showing the influences of heat generation, porous medium, viscous dissipation, temperature gradient, rate of mass diffusion and Joule heating.

It is remarked that the current study's findings are approximated using G-FEM. Table 4 shows a validation of results using the Nusselt number in the case of nanofluids (Table 5).

The Prandtl number decreases with the nano and hybrid particle volume fraction, whereas the Brownian motion parameter and the thermophoresis parameter increase with the nanoparticle volume fraction in Integral treatment for forced convection heat and mass transfer of nanofluids 300. It's interesting to note that the variation of the Lewis number has a varied pattern for different nanoparticles. In the case of Ag and Cu nano and hybrid nanoparticles, the Lewis number decreases as the nanoparticle volume percentage increases. As a result, for a

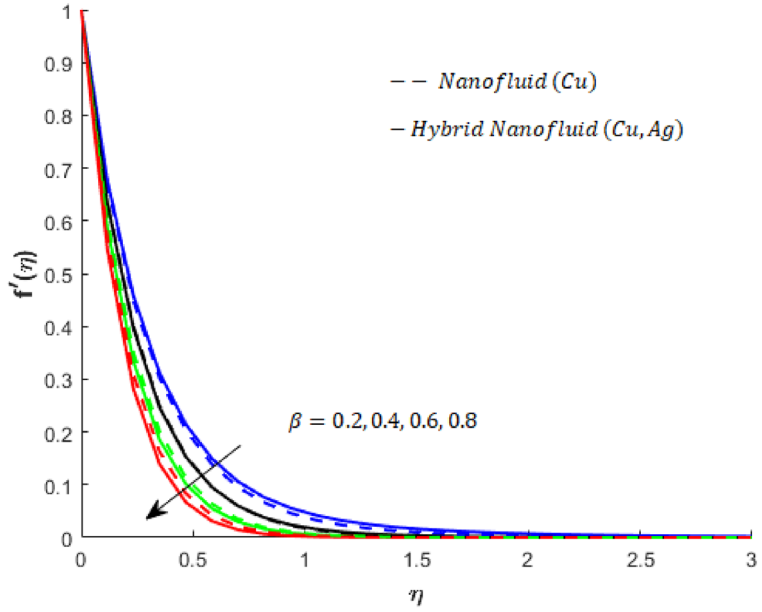

Figure 2. Influence of β on f' when $(Gr)_t = 0.5, Pr = 4, Sc = 5, K^* = 0.1, Ec = 0.001, (Gr)_c = 0.3, M = 0.5, \beta^* = 0.2, Sr = 0.1$ and $Du = 0.2$.

fixed reference temperature (T) and a specified size of nano and hybrid particles. Furthermore, the density of the nanoparticles is usually substantially higher than that of the basic fluid. As a result, adding heavy nanoparticles will increase the density of the resulting hybrid nanofluid, and increasing the volume fraction of nanoparticles will simultaneously increase the dynamic viscosity and density.

Results and discussion

The aspect of heat energy and mass diffusion in Newtonian fluid flow over a surface with temperature (variable) and wall concentration (variable) is modeled, and a coupled mathematical model is solved numerically using the G-FEM. The parameter β is called the flow fluid parameter; it determines the rheological behavior under yield stress. Yield stress is the characteristic by which fluid resists deformation until a certain amount of applied stress is reached. As the yield stress increases, the fluid's ability to resist the applied stress attains its equilibrium state; therefore, a decrease in the velocity field (in both the x and y components) is observed (see Figs. 2 and 3).

Various numerical experiments are performed with different samples of parametric values. Some crucial observations are obtained from the numerical experiments. It is important to note that dashed curves are associated with flow, heat transfer and mass diffusion in nanofluids (Cu-nanofluids), whereas solid curves are associated with flow, heat transfer and mass transport in hybrid nanofluids (Cu- Ag- nanofluids). The increase in the magnitude of the resistive force is captured first. Obviously, the flow in both the x- and y- directions decelerates; see Figs. 4 and 5). Moreover, the parameter k^* associated with porous medium resistivity against the flow of fluid and its impact on the motion of fluid particles is shown in Figs. 6, and 7 decreasing velocity behavior can be seen in Figs. 6 and 7. These figures also show that the hybrid nanofluid experiences more resistance to the porous medium than the mono nanofluid. The viscous region for nanofluids is wider than that for hybrid nanofluids.

Role of magnetic field versus fluid flow. The direct relation is addressed to the magnetic field and Lorentz force. The influence of the Lorentz force on flow can be determined by the variation in M. The large values of M increase the opposing effect of the Lorentzian force. Therefore, flow experiences retardation due to the Lorentz force. (See Figs. 6 and 7). Thus, BLT is approached by varying the magnetic field (the intensity of applied). It is also noted that the Lorentz force for the case of flow of the Cu- Ag- nanofluids is greater than the Lorentz force in the case of flow of the Cu-nanofluid.

Temperature field versus variation of crucial model parameters. The effects of Du, $(Gr)_t$, M, Pr, β^*, and Ec versus thermal energy for both nanofluids (Cu -nanofluids) and hybrid nanofluids (Cu- Ag- nanofluids) are examined. The observed influence of these parameters is shown in Figs. 8, 9. The parameter Du is called Dufour number. It appears in the dimensionless form of the energy equation when the transcript of thermal energy due to the concentration gradient is taken into account. It measures the transfer of heat energy due to compositional differences caused by nanoparticles and solute diffused in the fluid. The effects of Du on the temperature of the Cu -nanofluid and Cu- Ag- hybrid nanofluid are shown in Fig. 8. The temperature of both types of fluids has an increasing tendency as a function of Du. The influence of Du on the temperature of the Cu-nanofluid is smaller than that on the temperature of the Cu- Ag- nanofluids. The effects of the buoyancy force on the temperature of the Cu-nanofluid and Cu- Ag- nanofluids are represented by Fig. 9. $(Gr)_\in > 0$ is the case

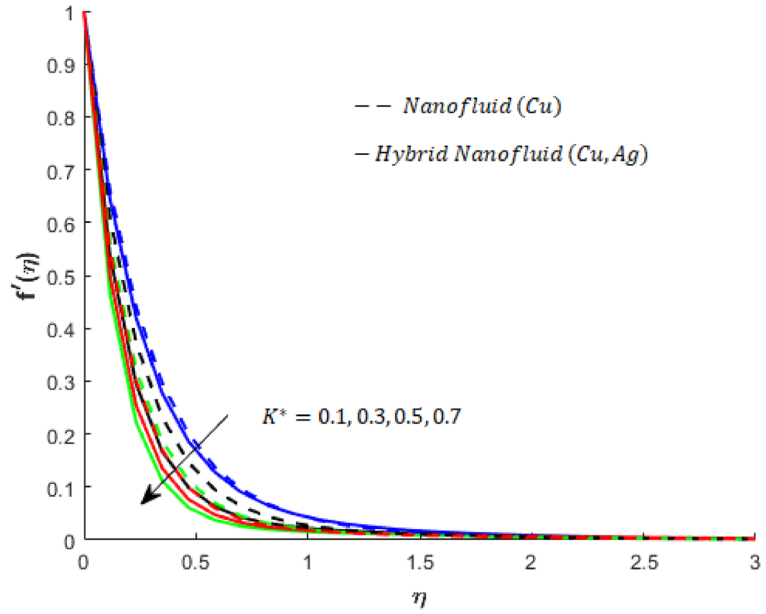

Figure 3. Influence of K^* on f' when $(Gr)_t = 0.5, Pr = 4, Sc = 5, \beta = 0.2, Ec = 0.001, (Gr)_c = 0.3, M = 0.5, \beta^* = 0.2, Sr = 0.1$ and $Du = 0.2$.

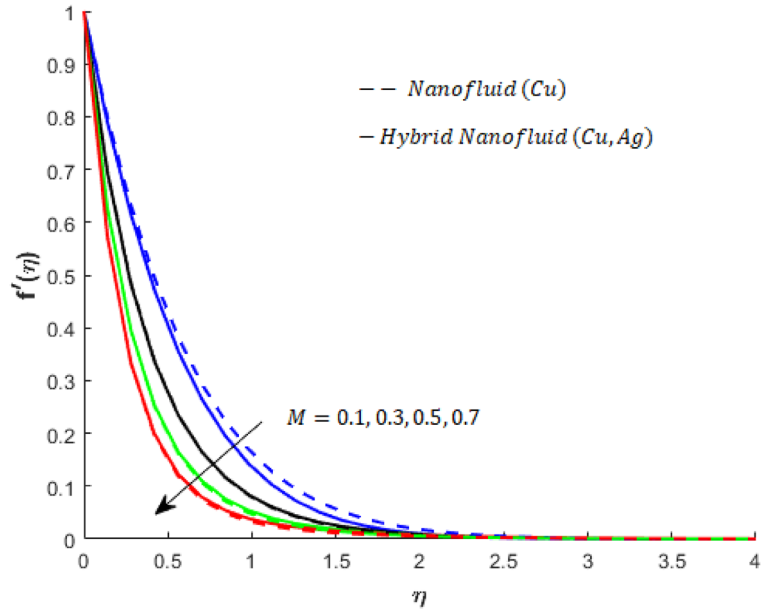

Figure 4. Influence of M on f' when $(Gr)_t = 0.5, Pr = 4, Sc = 5, \beta = 0.2, Ec = 0.001, (Gr)_c = 0.3, K^* = 0.1, \beta^* = 0.2, Sr = 0.1,$ and $Du = 0.2$

when the buoyancy force is positive, and flow is assisted by this force. However, $(Gr)_t < 0$ in the case when the buoyancy force is negative, the flow in this case is called opposing flow.

Wall shear stresses, heat transfer rate and mass flux. Numerical data related to wall shear stresses in the x and y-directions, wall heat transfer rate and wall mass flux for both types of fluids, Cu -fluid (mono nanofluid) and Cu -Ag -fluid (hybrid nanofluid), are investigated versus the variation in key parameters, k^*, Du, Sr and Sc (see Table 6). The numerical outcomes are summarized in Table 6. It appears that k^* is inversely proportional to the voids present in the porous medium. Hence, the resistive force per unit area (stress) increases. Therefore, wall shear stresses in both the x and y-directions are increasing functions of k^*. The temperature gradient and mass flux are both decreasing functions of k^*. It is also observed that wall shear stress increases when Du is increased. On the other hand, a rise in wall mass flux against Du is noted. Finally, the temperature gradient

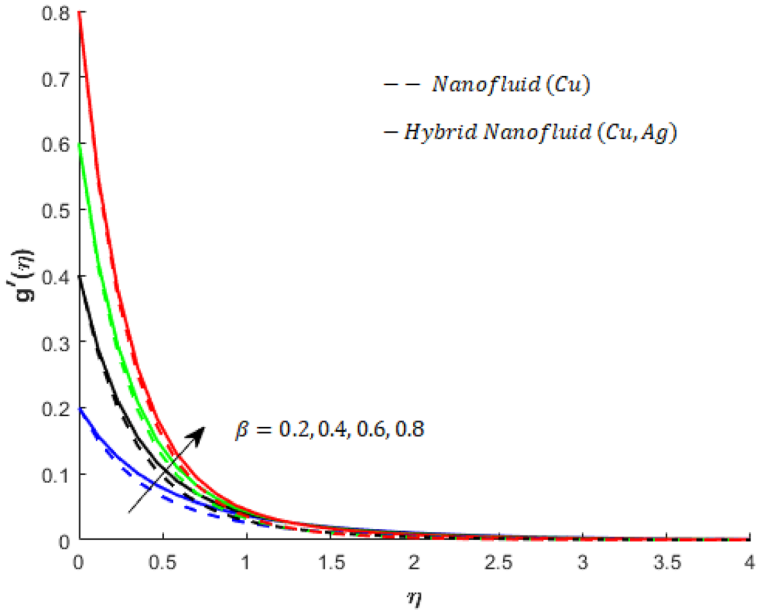

Figure 5. Influence of β on g' when $(Gr)_t = 0.5, Pr = 4, Sc = 5, K^* = 0.1, Ec = 0.001, (Gr)_c = 0.3, M = 0.5, \beta^* = 0.2, Sr = 0.1$ and $Du = 0.2$.

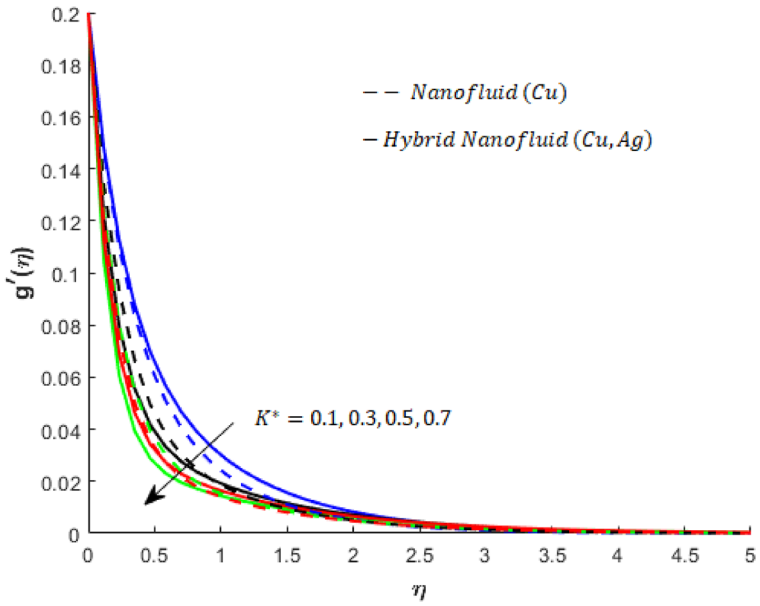

Figure 6. Influence of K^* on g' when $(Gr)_t = 0.5, Pr = 4, Sc = 5, \beta = 0.2, Ec = 0.001, (Gr)_c = 0.3, M = 0.5, \beta^* = 0.2, Sr = 0.1$ and $Du = 0.2$.

on solute particles is determined by Sr, and an increase in Sr causes a decrease in wall shear stress. However, the opposite trend is noted for Sc.

Core points and conclusions

The features of heat energy and mass diffusion, which play essential roles in the behaviour of nanoparticles and hybrid nanostructures, are addressed over the vertical 3D melting surface. Newtonian fluid is considered under simultaneous influences of heat generation, porous medium, viscous dissipation, temperature gradient, rate of mass diffusion, and Joule heating. The mathematical modelling is solved using the famous FEM. The prime findings are listed below:

1. The convergence of the proposed problem is confirmed for finite element mesh density equal to 300.

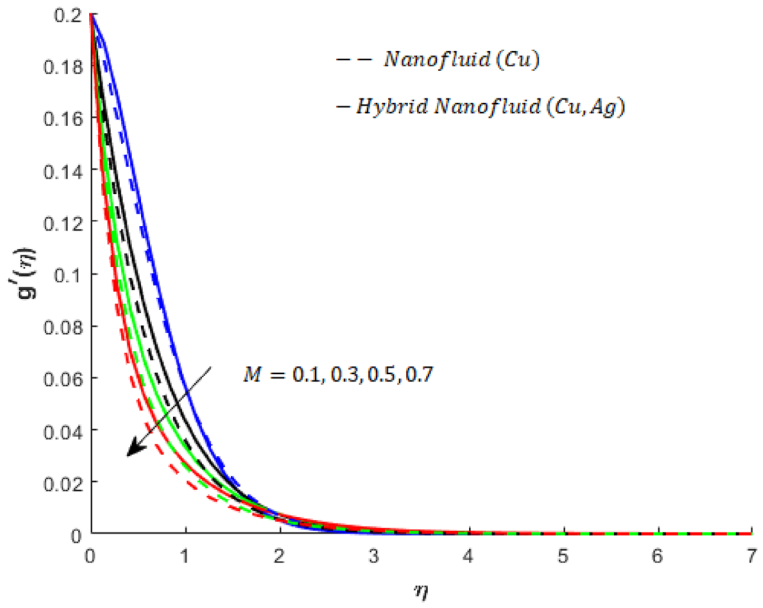

Figure 7. Influence of M on g' when $(Gr)_t = 0.5, Pr = 4, Sc = 5, \beta = 0.2, Ec = 0.001, (Gr)_c = 0.3, K^* = 0.1, \beta^* = 0.2, Sr = 0.1$ and $Du = 0.2$.

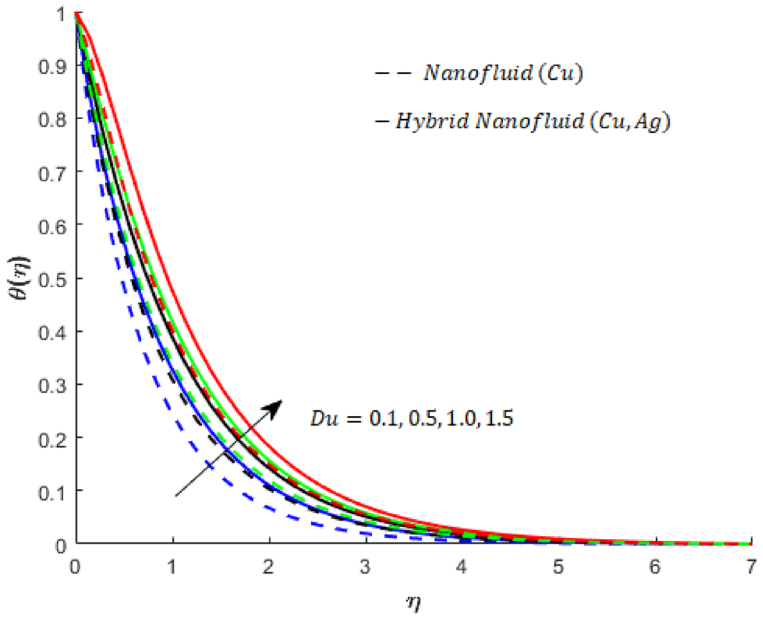

Figure 8. Influence of Du on θ when $(Gr)_t = 0.5, Pr = 4, Sc = 5, \beta = 0.2, Ec = 0.001, (Gr)_c = 0.3, K^* = 0.1, \beta^* = 0.2, Sr = 0.1$ and $M = 0.5$.

2. The magnetic field reduces the motion of both nanoparticles and hybrid nanostructures, where the effect on hybrid nanofluid is more significant than on nanofluid.
3. The Dufour number amplified the temperature of both hybrid nanofluid and nanofluid while the temperature for hybrid nanofluid is higher than nanofluid.
4. The temperature for both fluids diminish as the buoyancy force acts onto the system.
5. The joule heating parameter intensified the temperature for both fluids, and hybrid nanofluid is stronger than nanofluid.
6. The Prandtl number decreases the temperature profile for both fluids, but the temperature for hybrid nanofluid is slightly higher than nanofluid.
7. The temperature profile for both fluids increases when the heat generation and viscous dissipation act onto the system.

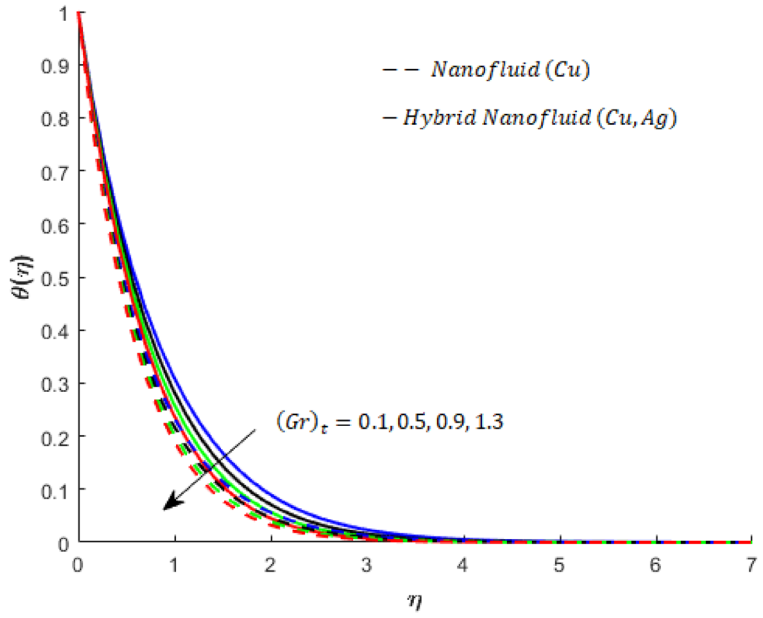

Figure 9. Influence of $(Gr)_t$ on θ when $Du = 0.2, Pr = 4, Sc = 5, \beta = 0.2, Ec = 0.001, (Gr)_c = 0.3, K^* = 0.1, \beta^* = 0.2, Sr = 0.1$ and $M = 0.5$.

		$C_{fx}(Re)^{1.5}$	$C_{fy}(Re)^{1.5}$	$Nu(Re)^{1.5}$	$Sh(Re)^{1.5}$
k^*	0.0	1.224110	1.512023	2.910831	2.7091217
	0.31	1.313851	1.712213	2.710327	2.5291402
	0.43	0.511053	1.913205	2.411028	2.3045191
	0.0	1.701101	1.514165	2.450237	2.512043
Du	0.4	1.512553	1.321243	2.703033	2.710017
	0.8	1.312105	1.215345	2.910211	2.915321
	0.0	1.537013	1.7060183	2.346892	3.3012731
Sr	0.3	1.303711	1.4139212	2.152565	3.1201361
	0.7	1.211321	1.3113031	2.511689	3.0231110
	0.0	1.211083	0.1280160	2.430243	2.3130353
Sc	0.5	1.501333	0.2150133	2.511035	2.4131321
	1.3	1.710150	0.3352120	2.710115	0.8153113

Table 6. Simulations of physical quantities when $Du = 0.2, M = 0.5, Sr = 0.1, \beta = 0.2, Pr = 4, (Gr)_c = 0.3, K^* = 0.1, \beta^* = 0.2, Ec = 0.001, Sc = 5$ and $(Gr)_t = 0.5$.

8. The temperature gradient increased the concentration for both fluids, while the diffusion parameter decreased the concentration for both fluids.
9. Wall shear stress amplified with the porous medium parameter, Dufour number and diffusion parameter but the wall shear stress decrease for the temperature gradient parameter. The mass wall flux rises with the Dufour number and decreases the wall shear stress, while heat transfer rate and mass flux decrease as the porous medium parameter increases.

The Galerkin finite element method could be applied to a variety of physical and technical challenges in the future[67–77].

Received: 17 December 2021; Accepted: 27 June 2022
Published online: 08 July 2022

References

1. Bergman, T. L., Lavine, A. S., Incropera, F. P. & DeWitt, D. P. *Introduction to Heat Transfer* (John Wiley & Sons, Hoboken, 2011).

2. Serrano, J., Olmeda, P., Arnau, F., Reyes-Belmonte, M. & Lefebvre, A. Importance of heat transfer phenomena in small turbochargers for passenger car applications. *SAE Int. J. Engines* **6**(2), 716–728 (2013).
3. Zhang, H. & Zhuang, J. Research, development and industrial application of heat pipe technology in China. *Appl. Therm. Eng.* **23**(9), 1067–1083 (2003).
4. Ramesh, K. N., Sharma, T. K. & Rao, G. A. P. Latest advancements in heat transfer enhancement in the micro-channel heat sinks: A review. *Arch. Comput. Methods Eng.* **28**(4), 3135–3165 (2021).
5. Zahra, E., Sheikholeslami, M., Farshad, S. A. & Shafee, A. Radiation heat transfer within a solar system considering nanofluid flow inside the absorber tube. *Int. J. Numer. Methods Heat Fluid Flow* **32**(2), 469–487 (2021).
6. Sheikholeslami, M. & Ganji, D. D. Ferrofluid convective heat transfer under the influence of external magnetic source. *Alex. Eng. J.* **57**(1), 49–60 (2018).
7. Zeeshan, A. & Bhargav, A. Thermal interfacial resistance and nanolayer effect on the thermal conductivity of Al_2O_3-CO_2 nanofluid: A molecular dynamics approach. arXiv preprint arXiv:2006.12805 (2020).
8. Sajjad, S. R., Hayat, T., Ellahi, R., Muhammad, T. & Alsaedi, A. Darcy–Forchheimer flow of nanofluid due to a curved stretching surface. *Int. J. Numer. Methods Heat Fluid Flow* **29**(1), 2–20 (2019).
9. Li, H., Ha, C. S. & Kim, I. Fabrication of carbon nanotube/SiO_2 and carbon nanotube/SiO_2/Ag nanoparticles hybrids by using plasma treatment. *Nanoscale Res. Lett.* **4**, 1384–1388 (2009).
10. Guo, S., Dong, S. & Wang, E. Gold/platinum hybrid nanoparticles supported on multiwalled carbon nanotube/silica coaxial nanocables: Preparation and application as electrocatalysts for oxygen reduction. *J. Phys. Chem. C* **112**, 2389–2393 (2008).
11. Makisima, A. Possibility of hybrids materials. *Ceram. Jpn.* **39**, 90–91 (2004).
12. Hayat, T. & Nadeem, S. Heat transfer enhancement with Ag–CuO/water hybrid nanofluid. *Res. Phys.* **7**, 2317–2324 (2017).
13. Selimefendigil, F. & Öztop, H. F. Mixed convection of nanofluids in a three-dimensional cavity with two adiabatic inner rotating cylinders. *Int. J. Heat Mass Transf.* **117**, 331–343 (2018).
14. Nabil, M. F. *et al.* Thermo-physical properties of hybrid nanofluids and hybrid nanolubricants: A comprehensive review on performance. *Int. Commun. Heat Mass Transf.* **83**, 30–39 (2017).
15. Minea, A. A. & El-Maghlany, W. M. Influence of hybrid nanofluids on the performance of parabolic trough collectors in solar thermal systems: Recent findings and numerical comparison. *Renew. Energy* **120**, 350–364 (2018).
16. Nazir, U., Sadiq, M. A. & Nawaz, M. Non-Fourier thermal and mass transport in hybridnano-Williamson fluid under chemical reaction in Forchheimer porous medium. *Int. Commun. Heat Mass Transf.* **127**, 105536 (2021).
17. Dogonchi, A. S., Divsalar, K. & Ganji, D. D. Flow and heat transfer of MHD nanofluid between parallel plates in the presence of thermal radiation. *Comput. Methods Appl. Mech. Eng.* **310**, 58–76 (2016).
18. Chamkha, A. J., Dogonchi, A. S. & Ganji, D. D. Magneto-hydrodynamic flow and heat transfer of a hybrid nanofluid in a rotating system among two surfaces in the presence of thermal radiation and Joule heating. *AIP Adv.* **9**(2), 025103 (2019).
19. Mosayebidorcheh, S., Sheikholeslami, M., Hatami, M. & Ganji, D. D. Analysis of turbulent MHD Couette nanofluid flow and heat transfer using hybrid DTM–FDM. *Particuology* **26**, 95–101 (2016).
20. Sheikholeslami, M., Kataria, H. R. & Mittal, A. S. Effect of thermal diffusion and heat-generation on MHD nanofluid flow past an oscillating vertical plate through porous medium. *J. Mol. Liq.* **257**, 12–25 (2018).
21. Nazir, U., Nawaz, M., Alqarni, M. M. & Saleem, S. Finite element study of flow of partially ionized fluid containing nanoparticles. *Arab. J. Sci. Eng.* **44**(12), 10257–10268 (2019).
22. Sajjad, S. R., Muhammad, T., Sadia, H. & Ellahi, R. Hydromagnetic flow of Jeffrey nanofluid due to a curved stretching surface. *Phys. A* **551**, 124060 (2020).
23. Bayones, F. S., Jamshed, W., Elhag, S. H. & Eid, M. R. Computational galerkin finite element method for thermal hydrogen energy utilization of first grade viscoelastic hybrid nanofluid flowing inside PTSC in solar powered ship applications. *Energy Environ.* 0958305X221081463 (2021).
24. Jamshed, W., Safdar, R., Brahmia, A., Alanazi, A. K., Abo-Dief, H. M. & Eid, M. R. Numerical simulations of environmental energy features in solar pump application by using hybrid nanofluid flow: Prandtl-eyring case. *Energy Environ.* 1–44 (2021).
25. Jamshed, W. *et al.* Thermal efficiency enhancement of solar aircraft by utilizing unsteady hybrid nanofluid: A single-phase optimized entropy analysis. *Sustain. Energy Technol. Assess.* **52**, 101898 (2021).
26. Jamshed, W. *et al.* A brief comparative examination of tangent hyperbolic hybrid nanofuid through a extending surface: Numerical Keller-Box scheme. *Sci. Rep.* **11**(1), 1–32 (2021).
27. Jamshed, W., Baleaznu, D., Mohd Nasir, N. A. A., Shahzad, F., Nisar, K. S., Shoaib, M., Ahmad, S. & Ismail, K. A. The improved thermal efficiency of Prandtl–Eyring hybrid nanofluid via classical Keller box technique. *Sci. Rep.* (2021).
28. Jamshed, W., Mohd Nasir, N. A. A., Qureshi, M. A., Shahzad, F., Banerjee, R., Eid, M. R., Nisar, K. S. & Ahmad, S. Dynamical irreversible processes analysis of Poiseuille magneto-hybrid nanofluid flow in microchannel: A novel case study. *Waves Random Complex Media* (2022).
29. Ouni, M., Ladhar, L. M., Omri, M., Jamshed, W. & Eid, M. R. Solar water-pump thermal analysis utilizing copper–gold/engine oil hybrid nanofluid flowing in parabolic trough solar collector: Thermal case study. *Case Stud. Therm. Eng.* **30**, 101756 (2022).
30. Jamshed, W. *et al.* Entropy amplified solitary phase relative probe on engine oil based hybrid nanofluid. *Chin. J. Phys.* **77**, 1654–1681 (2022).
31. Jamshed, W., Azeany Mohd Nasir, N. A., Brahmia, A., Nisar, K. S. & Eid, M. R. Entropy analysis of radiative [$MgZn_6$Zr-Cu/ EO] Casson hybrid nanoliquid with variant thermal conductivity along a stretching surface: Implementing Keller box method. In *Proceedings of the Institution of Mechanical Engineers, Part C* 1–20 (2022).
32. Bouslimi, J. *et al.* Dynamics of convective slippery constraints on hybrid radiative Sutterby nanofluid flow by Galerkin finite element simulation. *Nanotechnol. Rev.* **11**, 1219–1236 (2022).
33. Hayat, T. & Nawaz, M. Soret and Dufour effects on the mixed convection flow of a second-grade fluid subject to Hall and ion-slip currents. *Int. J. Numer. Meth. Fluids* **67**(9), 1073–1099 (2011).
34. Nawaz, M., Hayat, T. & Alsaedi, A. Dufour and Soret effects on MHD flow of viscous fluid between radially stretching sheets in porous medium. *Appl. Math. Mech.* **33**(11), 1403–1418 (2012).
35. Subrata, M., Shaw, S. & Shift, G. C. Fractional order model for thermochemical flow of blood with Dufour and Soret effects under magnetic and vibration environment. *Colloids Surf. B* **197**, 111395 (2021).
36. Iskandar, W., Ishak, A. & Pop, I. Dufour and Soret effects on Al_2O_3-water nanofluid flow over a moving thin needle: Tiwari and Das model. *Int. J. Numer. Methods Heat Fluid Flow* (2020).
37. Ambreen, K., Naeem, A. S., Ellahi, R., Sait, S. M. & Vafai, K. Dufour and Soret effects on Darcy-Forchheimer flow of second-grade fluid with the variable magnetic field and thermal conductivity. *Int. J. Numer. Methods Heat Fluid Flow* (2020).
38. Sheikholeslami, M. & Rashidi, M. M. Ferrofluid heat transfer treatment in the presence of variable magnetic field. *Eur. Phys. J. Plus* **130**, 115 (2015).
39. Ganguly, R., Sen, S. & Puri, I. K. Heat transfer augmentation using a magnetic fluid under the influence of a line dipole. *J. Magn. Magn. Mater.* **271**, 63–73 (2004).
40. Parsa, A. B., Rashidi, M. M., Bégc, O. A. & Sadri, S. M. Semi-computational simulation of magneto-hemodynamic flow in a semi-porous channel using optimal homotopy and differential transform methods. *Comput. Biol. Med.* **43**, 1142–1153 (2013).
41. Sheikholeslami, M. & Ellahi, R. Three-dimensional mesoscopic simulation of magnetic field effect on natural convection of nanofluid. *Int. J. Heat Mass Transf.* **89**, 799–808 (2015).

42. Zhang, X. & Huang, H. Effect of magnetic obstacle on fluid flow and heat transfer in a rectangular duct. *Int. J. Heat Mass Transf.* **51**, 31–38 (2014).
43. Sheikholeslami, M., Abelman, S. & Ganji, D. D. Numerical simulation of MHD nanofluid flow and heat transfer considering viscous dissipation. *Int. J. Heat Mass Transf.* **79**, 212–222 (2014).
44. Ghofrani, A., Dibaei, M. H., Hakim Sima, A. & Shafii, M. B. Experimental investigation on laminar forced convection heat transfer of ferrofluids under an alternating magnetic field. *Exp. Therm. Fluid Sci.* **49**, 193–200 (2013).
45. Sheikholeslami, M., Bandpy, M. G. & Vajravelu, K. Lattice Boltzmann simulation of magnetohydrodynamic natural convection heat transfer of Al_2O_3–water nanofluid in a horizontal cylindrical enclosure with an inner triangular cylinder. *Int. J. Heat Mass Transf.* **80**, 16–25 (2015).
46. Rashidi, M. M., Kavyani, N. & Abelman, S. Investigation of entropy generation in MHD and slip flow over a rotating porous disk with variable properties. *Int. J. Heat Mass Transf.* **70**, 892–917 (2014).
47. Jamshed, W. & Aziz, A. Entropy analysis of TiO_2-Cu/EG casson hybrid nanofluid via cattaneo-christov heat flux model. *Appl. Nanosci.* **08**, 01–14 (2018).
48. Hussain, S. M. & Jamshed, W. A comparative entropy based analysis of tangent hyperbolic hybrid nanofluid flow: Implementing finite difference method. *Int. Commun. Heat Mass Transf.* **129**, 105671 (2021).
49. Jamshed, W. *et al.* Thermal growth in solar water pump using Prandtl-Eyring hybrid nanofluid: A solar energy application. *Sci. Rep.* **11**(1), 1–21 (2021).
50. Hiba, B. *et al.* A novel case study of thermal and streamline analysis in a grooved enclosure filled with (Ag–MgO/Water) hybrid nanofluid: Galerkin FEM. *Case Stud. Therm. Eng.* **27**, 101372 (2021).
51. Jamshed, W. Thermal augmentation in solar aircraft using tangent hyperbolic hybrid nanofluid: A solar energy application. *Energy Environ.* 1–44 (2021).
52. Shahzad, F. *et al.* Thermal analysis on Darcy-Forchheimer swirling Casson hybrid nanofluid flow inside parallel plates in parabolic trough solar collector: An application to solar aircraft. *Int. J. Energy Res.* **45**(15), 20812–20834 (2021).
53. Jamshed, W. *et al.* Computational case study on tangent hyperbolic hybrid nanofluid flow: Single phase thermal investigation. *Case Stud. Therm. Eng.* **27**, 101246 (2021).
54. Jamshed, W., Nisar, K. S., Ibrahim, R. W., Shahzad, F. & Eid, M. R. Thermal expansion optimization in solar aircraft using tangent hyperbolic hybrid nanofluid: A solar thermal application. *J. Mater. Res. Technol.* **14**, 985–1006 (2021).
55. Ali, K. *et al.* Quasi-linearization analysis for heat and mass transfer of magnetically driven 3rd-grade (Cu-TiO_2/engine oil) nanofluid via a convectively heated surface. *Int. Commun. Heat Mass Transf.* **135**, 106060 (2022).
56. Jamshed, W. *et al.* Physical specifications of MHD mixed convective of Ostwald-de Waele nanofluids in a vented-cavity with inner elliptic cylinder. *Int. Commun. Heat Mass Transfer* **134**, 106038 (2022).
57. Bejawada, S. G. *et al.* 2D mixed convection non-Darcy model with radiation effect in a nanofluid over an inclined wavy surface. *Alex. Eng. J.* **61**, 9965–9976 (2022).
58. Hayat, T., Aziz, A., Muhammad, T. & Alsaedi, A. Darcy-Forchheimer flow of nanofluid in a rotating frame. *Int. J. Numer. Methods Heat Fluid Flow* (2018).
59. Hayat, T., Aziz, A., Muhammad, T. & Alsaedi, A. Three-dimensional flow of Prandtl fluid with Cattaneo-Christov double diffusion. *Res. Phys.* **9**, 290–296 (2018).
60. Ahmed, S. E. FEM-CBS algorithm for convective transport of nanofluids in inclined enclosures filled with anisotropic non-Darcy porous media using LTNEM. *Int. J. Numer. Methods Heat Fluid Flow* **31**(1), 570–594 (2020).
61. Ullah, N., Nadeem, S. & Khan, A. U. Finite element simulations for natural convective flow of nanofluid in a rectangular cavity having corrugated heated rods. *J. Therm. Anal. Calorim.* **143**(6), 4169–4181 (2021).
62. Khan, S. A., Nie, Y. & Ali, B. Multiple slip effects on MHD unsteady viscoelastic nanofluid flow over a permeable stretching sheet with radiation using the finite element method. *SN Appl. Sci.* **2**(1), 1–14 (2020).
63. Rehman, K. U., Qasem, M., Qaiser, A. A., Malik, M. Y. & Ahmed, M. N. Finite element examination of hydrodynamic forces in grooved channel having two partially heated circular cylinders. *Case Stud. Therm. Eng.* **18**, 100600 (2020).
64. Bagh, A., Rasool, G., Hussain, S., Baleanu, D. & Bano, S. Finite element study of magnetohydrodynamics (MHD) and activation energy in Darcy-Forchheimer rotating flow of Casson Carreau nanofluid. *Processes* **8**(9), 1185 (2020).
65. Nazir, U. *et al.* Inclusion of hybrid nanoparticles in hyperbolic tangent material to explore thermal transportation via finite element approach engaging Cattaneo-Christov heat flux. *PLoS ONE* **16**(8), 0256302 (2021).
66. Qureshi, I. H., Nawaz, M., Abdel-Sattar, M. A., Aly, S. & Awais, M. Numerical study of heat and mass transfer in MHD flow of nanofluid in a porous medium with Soret and Dufour effects. *Heat Transf.* **50**, 4501–4515 (2021).
67. Zhao, T. H., Khan, M. I. & Chu, Y. M. Artificial neural networking (ANN) analysis for heat and entropy generation in flow of non-Newtonian fluid between two rotating disks. *Math. Methods Appl. Sci.* (2021).
68. Zhao, T. H., He, Z. Y. & Chu, Y. M. On some refinements for inequalities involving zero-balanced hypergeometric function. *AIMS Math.* **5**(6), 6479–6495 (2020).
69. Zhao, T. H., Wang, M. K. & Chu, Y. M. A sharp double inequality involving generalized complete elliptic integral of the first kind. *AIMS Math.* **5**(5), 4512–4528 (2020).
70. Chu, Y. M., Nazir, U., Sohail, M., Selim, M. M. & Lee, J. R. Enhancement in thermal energy and solute particles using hybrid nanoparticles by engaging activation energy and chemical reaction over a parabolic surface via finite element approach. *Fractal Fract.* **5**(3), 17 (2021).
71. Chu, Y. M., Bashir, S., Ramzan, M. & Malik, M. Y. Model-based comparative study of magnetohydrodynamics unsteady hybrid nanofluid flow between two infinite parallel plates with particle shape effects. *Math. Methods Appl. Sci.* (2022).
72. Zhao, T. H., Chu, H. H. & Chu, Y. M. Optimal Lehmer mean bounds for the nth power-type Toader mean of n=-1, 1, 3. *J. Math. Inequal.* **16**(1), 157–168 (2022).
73. Zhao, T. H., Wang, M. K., Dai, Y. Q. & Chu, Y. M. On the generalized power-type Toader mean. *J. Math. Inequal.* **16**(1), 247–264 (2022).
74. Iqbal, S. A., Hafez, M. G., Chu, Y. M. & Park, C. Dynamical Analysis of nonautonomous RLC circuit with the absence and presence of Atangana-Baleanu fractional derivative. *J. Appl. Anal. Comput.* **12**(2), 770–789 (2022).
75. Ashpazzadeh, E., Chu, Y.-M., Hashemi, M. S., Moharrami, M. & Inc, M. Hermite multiwavelets representation for the sparse solution of nonlinear Abel's integral equation. *Appl. Math. Comput.* **427**, 127171 (2022).
76. Chu, Y. M. *et al.* Combined impact of Cattaneo-Christov double diffusion and radiative heat flux on bio-convective flow of Maxwell liquid configured by a stretched nano-material surface. *Appl. Math. Comput.* **419**, 126883 (2022).
77. Nazeer, M. *et al.* Theoretical study of MHD electro-osmotically flow of third-grade fluid in micro channel. *Appl. Math. Comput.* **420**, 126868 (2022).

Author contributions

M.B.H. and M.K. formulated and solved the problem. M.B.H., M.K., H.S., A.A.P. and M.A., computed and scrutinized the results. All the authors equally contributed in writing and proof reading of the paper. All authors reviewed the manuscript.

Competing interests
The authors declare no competing interests.

Additional information
Supplementary Information The online version contains supplementary material available at https://doi.org/10.1038/s41598-022-15560-5.

Correspondence and requests for materials should be addressed to M.B.H.

Reprints and permissions information is available at www.nature.com/reprints.

Publisher's note Springer Nature remains neutral with regard to jurisdictional claims in published maps and institutional affiliations.